

## ARTICLE OPEN



# Low Antarctic continental climate sensitivity due to high ice sheet orography

Hansi A. Singh<sup>1</sup>✉ and Lorenzo M. Polvani<sup>2</sup>

The Antarctic continent has not warmed in the last seven decades, despite a monotonic increase in the atmospheric concentration of greenhouse gases. In this paper, we investigate whether the high orography of the Antarctic ice sheet (AIS) has helped delay warming over the continent. To that end, we contrast the Antarctic climate response to CO<sub>2</sub>-doubling with present-day orography to the response with a flattened AIS. To corroborate our findings, we perform this exercise with two different climate models. We find that, with a flattened AIS, CO<sub>2</sub>-doubling induces more latent heat transport toward the Antarctic continent, greater moisture convergence over the continent and, as a result, more surface-amplified condensational heating. Greater moisture convergence over the continent is made possible by flattening of moist isentropic surfaces, which decreases humidity gradients along the trajectories on which extratropical poleward moisture transport predominantly occurs, thereby enabling more moisture to reach the pole. Furthermore, the polar meridional cell disappears when the AIS is flattened, permitting greater CO<sub>2</sub>-forced warm temperature advection toward the Antarctic continent. Our results suggest that the high elevation of the present AIS plays a significant role in decreasing the susceptibility of the Antarctic continent to CO<sub>2</sub>-forced warming.

*npj Climate and Atmospheric Science* (2020)3:39; <https://doi.org/10.1038/s41612-020-00143-w>

## INTRODUCTION

The impacts of anthropogenic greenhouse gas loading of the atmosphere are global, but nowhere are these changes more consequential than over the polar regions. Changes in polar climate have important impacts globally: ice sheet melt and polar ocean warming result in sea level rise<sup>1</sup>; warming and shifts in sea ice seasonality impact keystone species, like the Southern Ocean krill, which, in turn, impact the productivity of fisheries worldwide<sup>2</sup>; surface-amplified polar warming can shift the jet stream and storm tracks, effectively altering midlatitude climate variability<sup>3</sup>; and hemispherically asymmetric changes in polar ice cover, such as during the last glacial period, impact the position and intensity of the tropical rain belts<sup>4</sup>.

The polar regions, however, present a conundrum for understanding present-day climate change, as recent polar warming differs markedly between the Arctic and Antarctic. Over the past several decades, the Arctic has warmed rapidly<sup>5</sup>, a phenomenon linked to sea ice decline<sup>6,7</sup> and associated radiative feedbacks<sup>8–10</sup>. Indeed, the central Arctic has warmed by nearly 6 K over the last three decades<sup>11</sup>. Over the same period, Antarctic sea ice area has modestly expanded<sup>12</sup>, and warming has been nearly non-existent over much of the Antarctic ice sheet (AIS) (Fig. 1; also see ref. 13).

The orography of the AIS, which towers nearly 4 km above sea level at its highest, is possibly the most obvious factor which could account for weak (or non-existent) warming over the Antarctic continent. The presence of the AIS has a substantial impact on the mean state dynamics and thermodynamics of the Southern Hemisphere (see, e.g., 14–19). Global climate model (GCM) experiments in which Antarctic continental orography is flattened exhibit weaker baroclinicity over the Southern Ocean, greater baroclinicity over the Antarctic continent, and, consequently, more frequent incursion of midlatitude eddies over the Antarctic plateau<sup>14,20,21</sup>. At the same time, (equatorward) katabatic flow away from the Antarctic continent ceases when Antarctic

orography is flattened, and the Southern hemispheric polar cell vanishes<sup>15,16</sup>.

Taken together, these factors imply a greater (moist and dry) atmospheric energy transport toward the Antarctic continent when orography is flattened<sup>22</sup>. In a warmer CO<sub>2</sub>-forced world, such factors would be expected to further enhance energy transport toward the Antarctic continent, as a consequence of increased atmospheric sensible and latent heat content. These considerations suggest that the presence or absence of Antarctic orography may considerably affect the local Antarctic continental warming in response to increased CO<sub>2</sub>.

Recently, a single coarse-resolution GCM was used to investigate the impact of AIS orography on warming over the Antarctic continent with CO<sub>2</sub>-doubling<sup>23</sup>. While reporting that the CO<sub>2</sub>-forced lapse rate feedback over the Antarctic continent increased significantly when Antarctic orography was flattened, implying an increase in surface-amplified warming, that study did not address which dynamical mechanisms may trigger such an increase, nor the robustness of that increase in the lapse rate feedback.

In the present study, we address these questions. We use two state-of-the-art GCMs—with different physical parameterizations and different equilibrium climate sensitivities—to show that when CO<sub>2</sub> is doubled, the orography of the present-day AIS shields the Antarctic continent from dynamic extrapolar transport processes that might otherwise warm it. When the orography of the AIS is flattened, we show that these shielding mechanisms are no longer at play, and winter season surface-amplified warming with CO<sub>2</sub>-doubling is significantly greater. As expected, we find that such a dynamically driven increase in surface-amplified warming augments the lapse rate feedback over the Antarctic continent. Our results imply that the high orography of Antarctica constitutes a significant local dynamical barrier to CO<sub>2</sub>-induced surface warming, both today and in the near future, provided orographic changes remain small.

<sup>1</sup>University of Victoria, School of Earth and Ocean Sciences, Victoria, BC, Canada. <sup>2</sup>Columbia University, Department of Applied Physics and Applied Mathematics, and Department of Earth and Environmental Sciences, New York City, NY, USA. ✉email: [hansingh@uvic.ca](mailto:hansingh@uvic.ca)

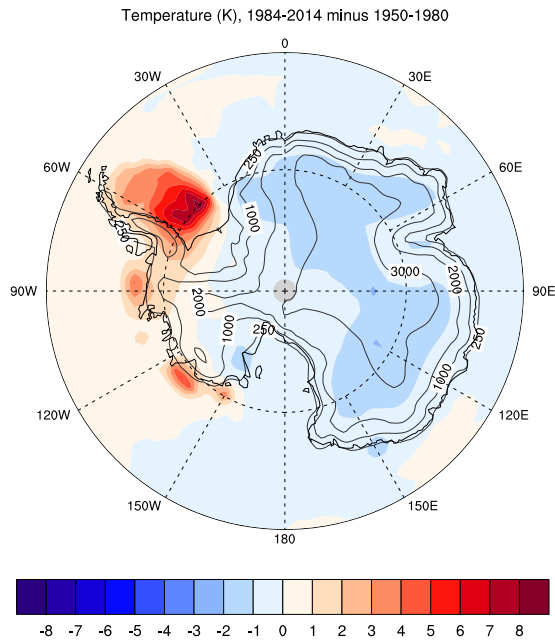


**Fig. 1 Observed surface temperature anomaly.** Mean surface temperature anomaly over years 1984–2014 (compared to the base period 1950–1980) over the Antarctic from the NOAA-MLOST regrided temperature product<sup>11</sup>. Contours show the surface elevation above sea level (in m).

## RESULTS

### Antarctic response to CO<sub>2</sub>-doubling with flattened orography

The key finding of this study is that in response to atmospheric CO<sub>2</sub>-doubling, warming over the Antarctic continent is significantly greater with flattened orography than with present-day orography in both CESM1.1 and CCSM4.0 (Fig. 2a; compare red and blue bars). Warming is greater in the annual mean (0.9 K greater in CCSM4.0 and 0.7 K greater in CESM1.1) because of significantly greater warming over winter (June–July–August (JJA); 1.5 K and 1.2 K greater warming in CCSM4.0 and CESM1.1, respectively) and the shoulder seasons (March–April–May (MAM) and September–October–November (SON); 1.4 K and 1.1 K greater warming in MAM in CCSM4.0 and CESM1.1, respectively, and 0.8 K and 0.4 K greater warming in SON in CCSM4.0 and CESM1.1, respectively). In both models, CO<sub>2</sub>-induced warming in the present-day and flattened orography runs is comparable in summer (DJF).

The amplified warming over the Antarctic continent with flattened orography is also evident in Fig. 2b, where we compare Antarctic amplification, defined as the ratio between surface warming over the Antarctic continent and warming over the globe, in the present-day and flattened Antarctic orography experiments. In the annual mean, we find greater amplification of CO<sub>2</sub>-forced warming over the Antarctic continent with flattened orography than with present-day orography: the Antarctic amplification ratio increases from 1.5 to 1.9 in CESM1.1, and from 1.4 to 1.5 in CCSM4.0. Seasonally, greater Antarctic amplification with flattened orography is most prominent in winter (JJA), when the Antarctic amplification ratio increases from 1.6 to 2.2 in CESM1.1, and from 1.4 to 1.8 in CCSM4.0. Increased CO<sub>2</sub>-forced Antarctic amplification with flattened orography is also evident in the shoulder seasons, though it is stronger in fall (MAM; increases from 1.7 to 2.3 in CESM1.1, and from 1.5 to 1.8 in CCSM4.0) and weaker in spring (SON; increases from 1.4 to 1.7 in CESM1.1, and from 1.3 to 1.4 in CCSM4.0). We note that while both models are in qualitative agreement, there are considerable

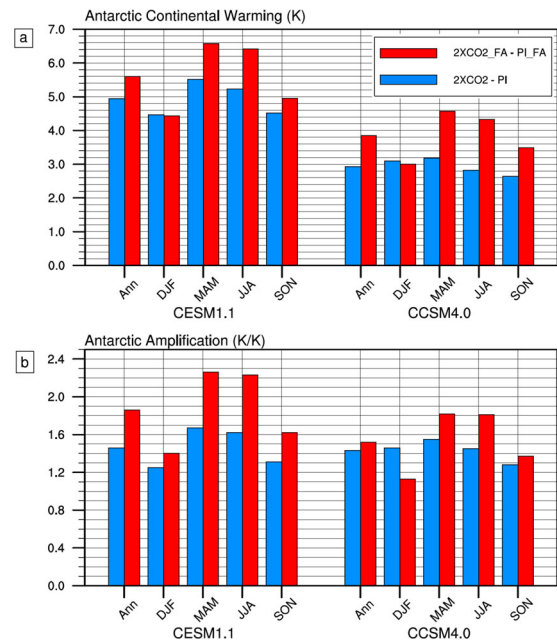


**Fig. 2 Antarctic (annual and seasonal) surface temperature change and amplification with CO<sub>2</sub>-doubling.** Annual mean and seasonal (December–January–February, DJF; March–April–May, MAM; June–July–August, JJA; and September–October–November, SON) area-weighted **a** surface temperature change over the Antarctic continent with CO<sub>2</sub>-doubling, and **b** the Antarctic amplification, the ratio of the Antarctic continental temperature change and the global surface temperature change with CO<sub>2</sub>-doubling. Shown for the (left) CESM1.1 and (right) CCSM4.0.

quantitative discrepancies, implying that single model studies must be treated with caution.

Since it is clear that both greater Antarctic amplification and greater CO<sub>2</sub>-forced warming over the Antarctic continent with flattened orography are most prominent in winter (JJA), for the remainder of this study we focus on this season, as we analyze the Antarctic continental warming and bring to light the mechanisms responsible for it.

In Fig. 3, we present the spatial pattern of winter season Antarctic surface warming in CESM1.1 and CCSM4.0. In both models, increased CO<sub>2</sub>-forced surface warming with flattened Antarctic orography is greatest over the West Antarctic Ice Sheet and Peninsula, and smallest over regions of the East Antarctic. In CESM1.1, West Antarctic warming extends into the Western Pacific Ocean Sector of the East Antarctic, while in CCSM4.0, warming extends in the opposite direction into the Weddell Sea Sector. Over some areas of the West Antarctic, winter season warming is nearly 5 K greater—in both models—when Antarctic orography is flattened. The spatial pattern of Antarctic surface warming in the winter season resembles that in the annual mean (compare Fig. 3 to Supplementary Fig. 1), suggesting that winter season processes drive the annual mean signal.

To understand why CO<sub>2</sub>-forced warming over the Antarctic continent is greater with flattened orography than with present-day orography, we now examine how (moist and dry) transport processes into the Antarctic respond differently to CO<sub>2</sub>-doubling in the two cases.

### Increased moisture advection with flattened orography

It is well-known that when forced with CO<sub>2</sub>, nearly all climate models respond with an increase in poleward latent heat transport<sup>24</sup>: this is clearly seen in our runs with CESM1.1 and CCSM4.0 (Fig. 4, solid blue lines). Such increased poleward latent

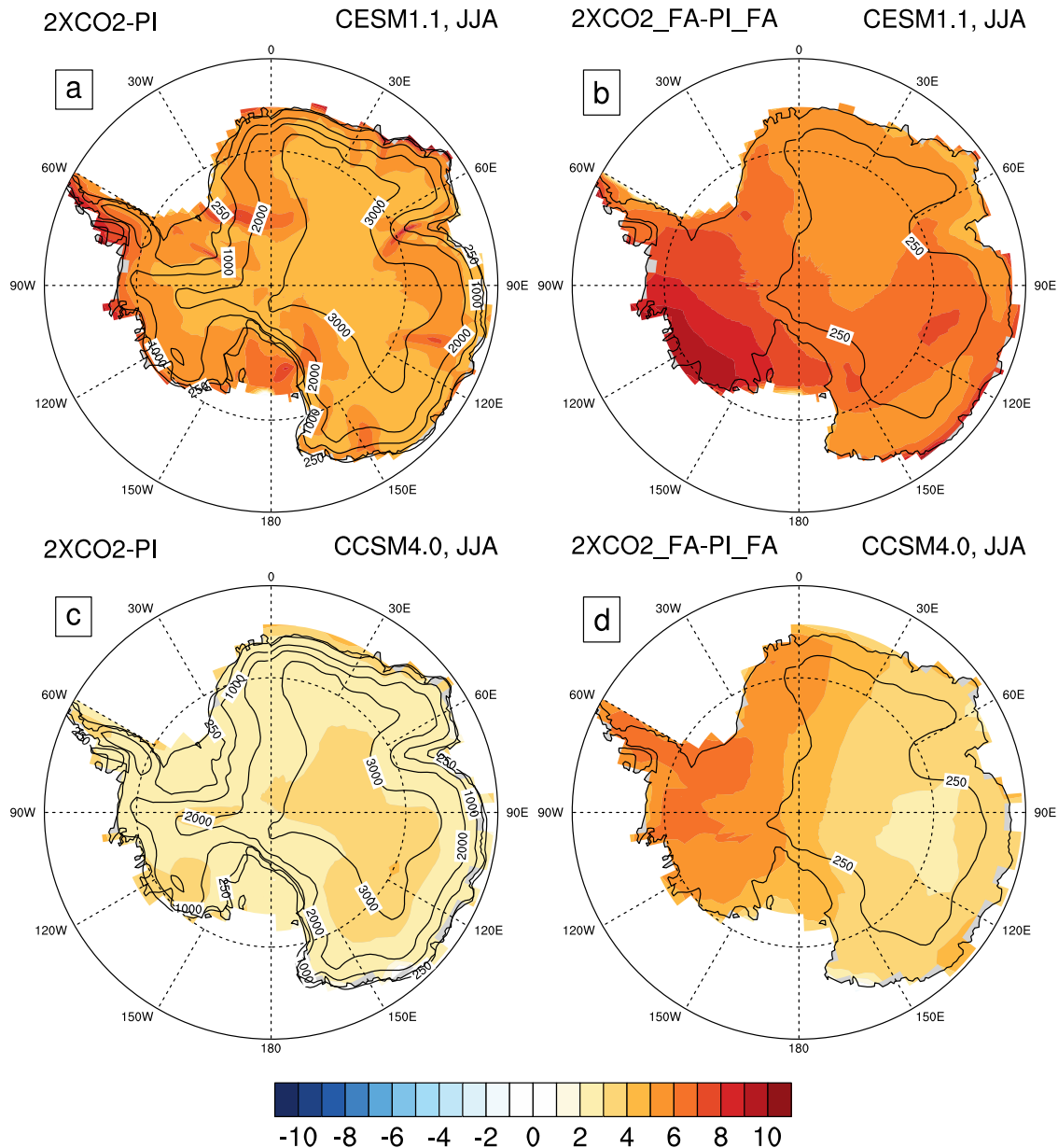


**Fig. 3 Antarctic winter season surface temperature change with CO<sub>2</sub>-doubling.** Winter season surface temperature change over the Antarctic continent (in K; colors) with CO<sub>2</sub>-doubling in the **a, b** CESM1.1 and **c, d** CCSM4.0 when **a, c** Antarctic orography is at its present-day height, 2 × CO<sub>2</sub> minus PI, and when **b, d** Antarctic orography is flattened to 10% of its present-day height, 2 × CO<sub>2</sub>\_FA minus PI\_FA. Contours show the surface elevation (in m).

heat transport is expected on theoretical grounds, since atmospheric specific humidity depends exponentially on temperature through the Clausius–Clapeyron relation, which enhances the meridional gradient of precipitable water in a warmer world<sup>25</sup>. Conversely, poleward dry static energy transport declines in many models with CO<sub>2</sub> forcing<sup>24</sup>, including CESM1.1 and CCSM4.0 (Fig. 4, pink lines), since polar-amplified warming weakens the meridional temperature gradient.

When Antarctic orography is flattened, we find a larger increase in CO<sub>2</sub>-forced latent heat transport toward the Antarctic continent than when orography is at its present-day height. This is evident in both CESM1.1 and CCSM4.0 (Fig. 4, panels a and b, respectively; compare solid and dashed blue lines), corresponding to a 0.05 PW increase in latent heat transport across 70S in both models; this represents a 100% increase in the poleward latent heat transport

response to CO<sub>2</sub>-doubling in CCSM4.0, and a 50% increase in CESM1.1.

To understand why latent heat transport at high Southern latitudes increases more with CO<sub>2</sub> forcing when Antarctic orography is flattened, we consider the spatial structure of the moist isentropes (isolines of both the equivalent potential temperature,  $\theta_E$ , and the MSE) in both flattened and present-day Antarctic orography experiments (Fig. 5). In the latitude-height plane, flattened Antarctic orography is associated with flattened moist isentropes over the pole, compared to present-day Antarctic orography where isentropes are more sloped (compare, for example, the 270 K moist isentrope in Fig. 5, panels a, c with those in panels b, d); this is true whether atmospheric CO<sub>2</sub> is at preindustrial concentrations (Fig. 5, black contours) or doubled (Fig. 5, red contours).

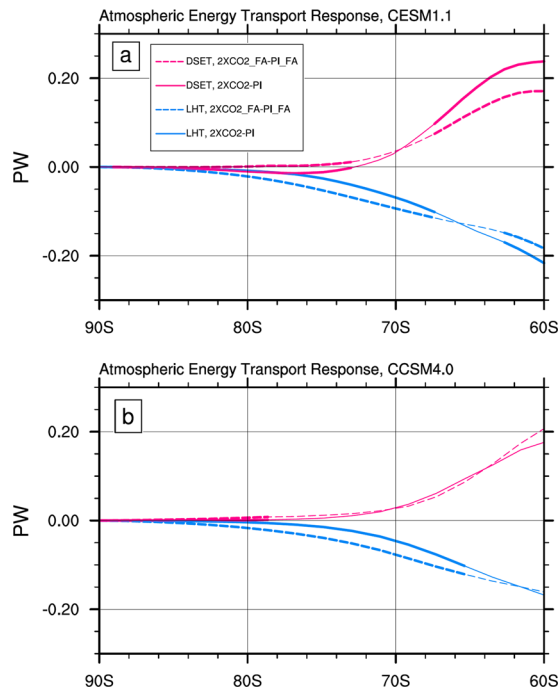


**Fig. 4 Atmospheric energy transport response to CO<sub>2</sub>-doubling.** Change in the northward dry static energy transport (DSET; pink lines) and latent heat transport (LHT; blue lines), in PW, with CO<sub>2</sub>-doubling in **a** CESM1.1 and **b** CCSM4.0. The atmospheric energy transport response to CO<sub>2</sub>-doubling is shown when Antarctic orography is in its present-day elevation (solid lines), and when Antarctic orography is flattened to 10% of its present-day height (dashed lines). Thick lines show where the (dry and moist) energy transport responses to CO<sub>2</sub>-doubling are statistically distinct (at  $p < 0.05$ ) between the present-day and flattened orography experiments.

In the extratropics, moist isentropes effectively act as isolines of the poleward moisture transport streamfunction<sup>26,27</sup>, particularly for moisture transport to the Antarctic continent<sup>28</sup>. The moist static energy (MSE), the sum of atmospheric latent heat, sensible heat, and geopotential, is conserved along a moist isentrope, and can be written as

$$MSE = L_v q + C_p T + g\Phi, \quad (1)$$

where  $L_v$  is the latent heat of fusion,  $q$  is the specific humidity,  $C_p$  is the specific heat of dry air at constant pressure,  $T$  is the temperature,  $g$  is the acceleration due to gravity, and  $\Phi$  is the height relative to the geoid. When moist isentropes are flatter (as when Antarctic orography is flattened), air parcels gain less geopotential as they flow poleward, and therefore retain more moisture. This is also evident in the change in specific humidity with CO<sub>2</sub>-doubling (Fig. 5, colors): the (poleward) gradient of this specific humidity change along a moist isentropic surface,  $\nabla(\Delta q)|_{\theta_E}$ , is greater with present-day Antarctic orography (panels a, c) than with flattened Antarctic orography (panels b, d), indicating that more moisture is lost along this trajectory with present-day orography than with flattened orography (compare, for example, the gradient of the change in specific humidity, denoted by the blue colors, along the 270 K moist isentrope in Fig. 5a, c with those in 5b, d).

As poleward latent heat transport towards the Antarctic continent increases more in response to CO<sub>2</sub>-doubling when Antarctic orography is flattened (see Fig. 4), condensational heating in the boundary layer over Antarctica also increases more: this is seen by comparing the left and right columns in Fig. 6, where condensational heating has been calculated in the lowest

200 hPa of the atmospheric column. Flattening of moisture transport trajectories (by flattening moist isentropes, see Fig. 6) results in less condensational depletion of poleward-moving moisture at the edge of the continent, thereby permitting more moisture to condense over the continental interior. Similarly, when Antarctic orography is flattened, CO<sub>2</sub>-forced precipitation increases are smaller over the edge of the Antarctic continent, and significantly greater over the continental interior (see Supplementary Fig. 2). In both CCSM4.0 and CESM1.1 flattened orography experiments, the increase in condensational heating in the boundary layer with CO<sub>2</sub>-doubling approximately occurs over the same regions where CO<sub>2</sub>-forced temperature increases are greatest (particularly over the West Antarctic in both models; compare Fig. 3a, b to Fig. 6a, b), indicating that condensational heating plays a key role in warming these regions.

#### Increased sensible heat advection with flattened orography

While greater moisture transport amplifies CO<sub>2</sub>-forced warming over the Antarctic continent when Antarctic orography is flattened, dry processes also contribute to greater warming. Previous studies on how flattened Antarctic orography impacts the mean state climate suggest a range of local changes in the atmospheric circulation, including weakening of the polar vortex<sup>14,17</sup>, slowing of the eddy-driven jet<sup>14,16,22</sup>, increased baroclinicity closer to the pole<sup>14,21</sup> and a cessation of katabatic flow over the continent<sup>15,16,18</sup>. In both CCSM4.0 and CESM1.1, the latter is associated with the disappearance of the polar cell in the mass overturning streamfunction when orography is flattened (Fig. 7, compare contours in panels a, c with b, d; also see refs. <sup>15,22</sup>).

The presence (or absence) of the polar cell determines how meridional temperature advection responds to CO<sub>2</sub>-doubling over the high Southern latitudes. When Antarctic orography is at present-day height, the temperature advection response is northward in the lower troposphere (Fig. 7a, c, colors), as warm temperature anomalies are advected away from the Antarctic continent by the lower branch of the polar cell. When Antarctic orography is flattened, on the other hand, the meridional temperature advection response is towards the continent (i.e., southward; Fig. 7b, d, colors) in the lower troposphere, as warmer boundary layer air from areas where sea ice has retreated is more readily advected poleward when the polar cell is absent.

Previous studies have shown that CO<sub>2</sub>-forced GCMs simulate similar advection of lower tropospheric warm anomalies from newly ice-free ocean regions in the Arctic to adjacent land regions: while summer season sea ice decline and ocean mixed layer warming in the Arctic directly cause (delayed) surface-amplified warming over the Arctic Ocean in fall and winter<sup>7</sup>, warming over boreal land regions is primarily through warm air advection from the polar oceans<sup>29</sup>. Therefore, when Antarctic orography is flattened, there is greater similarity between the poles in how advection of boundary layer air from newly ice-free ocean waters warms land areas in winter.

#### Greater surface-amplified warming with flattened orography

As a result of both the dry and moist transport processes described above, Antarctic continent surface temperatures warm more with CO<sub>2</sub>-doubling when Antarctic orography is flattened (recall Figs. 2 and 3).

The overlying atmosphere also warms with CO<sub>2</sub>-doubling, and that warming is also more surface-amplified with flattened Antarctic orography than with present-day orography (Fig. 8, compare red with black lines). As we have shown, such surface-amplified warming is a result of greater atmospheric energy transport convergence (both dry and moist) into the lower troposphere when Antarctic orography is flattened, combined with strong atmospheric static stability in winter which prevents

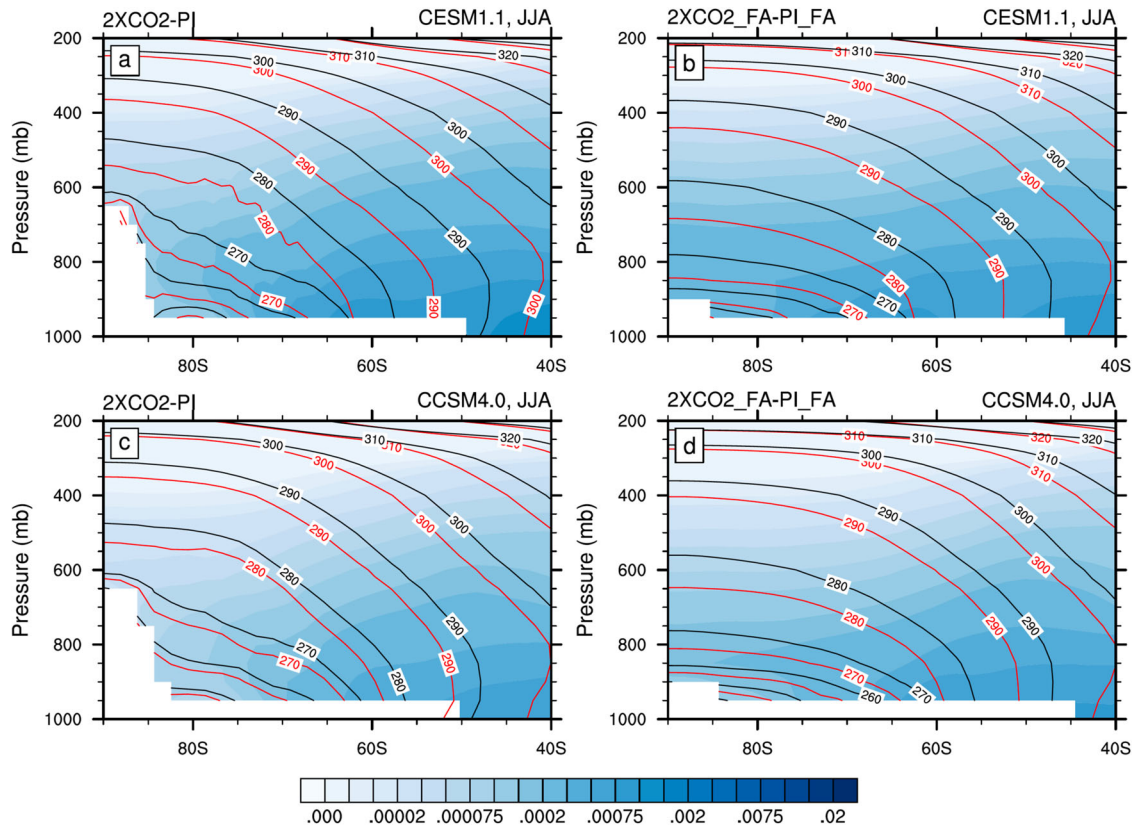


**Fig. 5** Moist isentropic surfaces and atmospheric specific humidity change with CO<sub>2</sub>-doubling. Mean moist entropy (contours; in K) and the change in the atmospheric specific humidity with CO<sub>2</sub>-doubling (shading; in kg per kg) in the **a, b** CESM1.1 and **c, d** CCSM4.0. Shown **a, c** when Antarctic orography is at its present-day height and **b, d** when Antarctic orography is flattened to 10% of its present-day height. The contours of moist entropy are shown for the corresponding pre-industrial experiment (i.e., PI or PI\_FA; in black) and the CO<sub>2</sub>-doubling experiment (i.e., 2 × CO<sub>2</sub> or 2 × CO<sub>2</sub>\_FA; in red).

convective transfer of these anomalies aloft (recall the stable stratification implied by moist isentropes in Fig. 4; also see ref. <sup>30</sup>).

Greater surface-amplified warming with CO<sub>2</sub>-doubling when Antarctic orography is flattened also leads to a stronger (positive) lapse rate feedback over the Antarctic continent itself: 1.2 W/m<sup>2</sup>/K (0.8 W/m<sup>2</sup>/K) with flattened Antarctic orography compared to 0.5 W/m<sup>2</sup>/K (0.3 W/m<sup>2</sup>/K) with present-day Antarctic orography in CESM1.1 (CCSM4.0), which we have computed using the radiative kernel method<sup>31</sup> with a CAM3-derived temperature kernel<sup>32</sup>. The positive lapse rate feedback in the high latitudes is one of the most important radiative factors responsible for polar-amplified warming in response to CO<sub>2</sub> forcing, particularly that of the Arctic<sup>9,10,30,33,34</sup>. Its increase when Antarctic orography is flattened is consistent with the increase in Antarctic (continental) amplification reported here (recall Fig. 2).

## DISCUSSION

In this study, we have used two state-of-the-art GCMs to show that Antarctic ice sheet orography robustly decreases climate sensitivity over the Antarctic continent, and that a flattened Antarctic ice sheet would experience significantly greater surface warming than the present-day Antarctic ice sheet. When CO<sub>2</sub> is doubled, we have shown that both moist and dry dynamic processes are more efficient at warming a flattened Antarctic continent. These dynamic processes differ from those that occur when Antarctica is at its present-day elevation because the presence of Antarctic orography significantly alters the atmospheric circulation at high Southern latitudes (see, e.g., <sup>14–16</sup>); differences in the unperturbed

circulation due to differences in orography result in different (moist and dry transport) responses to CO<sub>2</sub>-doubling.

Over the Antarctic continent, our results generally agree with those of ref. <sup>23</sup>, who also found greater surface-amplified warming over the Antarctic continent (and, therefore, a more positive lapse rate feedback) with CO<sub>2</sub>-doubling when Antarctic orography is flattened. In our study, we have specifically identified a number of atmospheric processes which act to increase CO<sub>2</sub>-forced surface-amplified warming (and, hence, the lapse rate feedback) over the Antarctic continent when its orography is flattened. We suggest that these mechanisms are robust because they depend upon changes in atmospheric circulation with Antarctic orography flattening that are consistent across a broad range of GCMs of varying complexity (see, e.g., <sup>14,17,19,21,22</sup>).

Unlike<sup>23</sup>, we do not find that annual mean Antarctic surface warming with CO<sub>2</sub>-doubling exceeds that over the Arctic when Antarctic orography was flattened in either of the models we studied (see Supplementary Fig. 3). In fact, our two models disagree on the impact of Antarctic orography flattening on Arctic warming: CCSM4.0 shows more Arctic warming with CO<sub>2</sub>-doubling when Antarctic orography is flattened, while CESM1.1 shows less. Therefore, the Arctic response to a flattened AIS does not appear to be robust. In addition, we find that the remote (atmospheric and oceanic) energy transport response to CO<sub>2</sub>-doubling when Antarctic orography is flattened, reported by<sup>23</sup>, is also not robust (see Supplementary Fig. 4). Specifically, CCSM4.0 shows a greater increase in ocean heat transport into the Arctic with CO<sub>2</sub>-doubling when Antarctic orography is flattened, whereas CESM1.1 shows a smaller increase; these transport responses are consistent with increased Arctic warming in the former and decreased Arctic

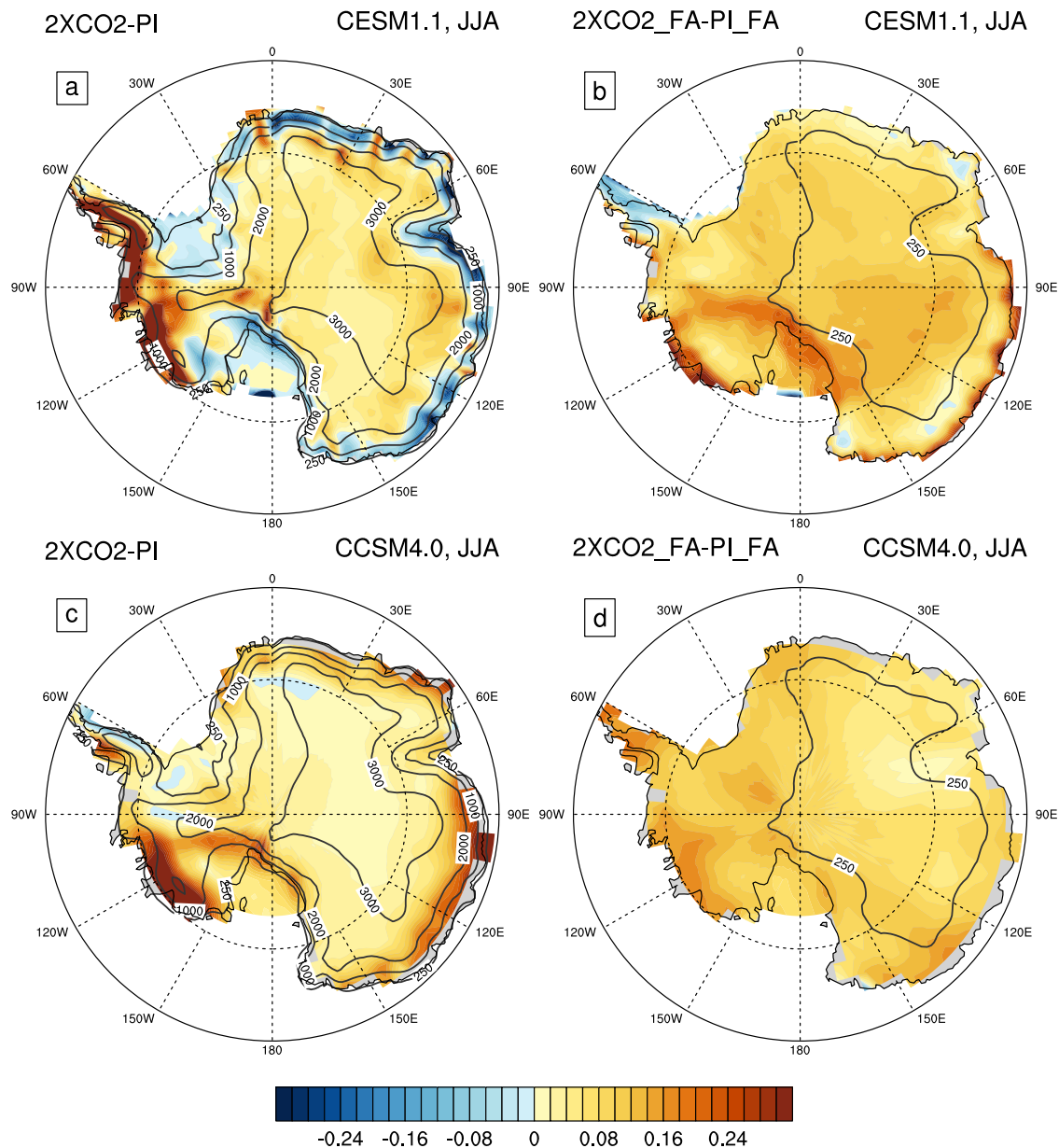


**Fig. 6 Condensational heating change with CO<sub>2</sub>-doubling.** Change in the lower tropospheric (lowest 200 hPa) condensational heating rate over the Antarctic continent (in K per day; colors) with CO<sub>2</sub>-doubling in the **a, b** CESM1.1 and **c, d** CCSM4.0 when **a, c** Antarctic orography is at its present-day height, 2 × CO<sub>2</sub> minus PI, and when **b, d** Antarctic orography is flattened to 10% of its present-day height, 2 × CO<sub>2</sub>\_FA minus PI\_FA. Contours show the surface elevation (in m).

warming in the latter (increased ocean heat convergence increases polar warming; see, e.g.,<sup>35,36</sup>).

In this study, we've identified Antarctic orography as one of (likely) several factors that reduces the magnitude of CO<sub>2</sub>-forced warming over the Antarctic continent. Further factors may also be responsible for a weak climate change signal over the Antarctic continent, including heat uptake by the Southern Ocean<sup>37</sup> and the meagre decline of Antarctic sea ice (in both observations and future GCM projections; see refs.<sup>12,38</sup>). More research is necessary to identify the extent to which warming or cooling over the open Southern Ocean and sea ice zones impacts surface temperatures over high-elevation regions of the Antarctic ice sheet, as the dynamics of the extratropical atmosphere suggests that these regions should be relatively isolated from adjacent low-elevation regions<sup>28,39,40</sup>. Our experiments, for example, show that differences in sea ice loss and warming over the marginal ice zone are

not primarily responsible for greater warming over the flattened Antarctic continent. In fact, CESM1.1 simulates less Antarctic sea ice retreat with CO<sub>2</sub>-doubling when Antarctica is flattened whereas CCSM4.0 simulates more Antarctic sea ice retreat (see Supplementary Fig. 5), even though both models simulate greater warming over the continent (recall Figs. 2 and 3).

For the sake of completeness, we also remind the reader that other factors have been suggested to have contributed to the absence of warming over the Antarctic continent in the past several decades, but these suggestions have been shown to be off target. For instance, on the basis of idealized model runs<sup>41</sup>, it was suggested that the formation of the ozone hole over the South pole, which has caused the majority of the positive trends in the Southern Annual Mode with accompanying surface wind stress changes<sup>42</sup>, could have contributed to colder SSTs and increased sea ice extent around Antarctica<sup>43</sup>. However, numerous studies

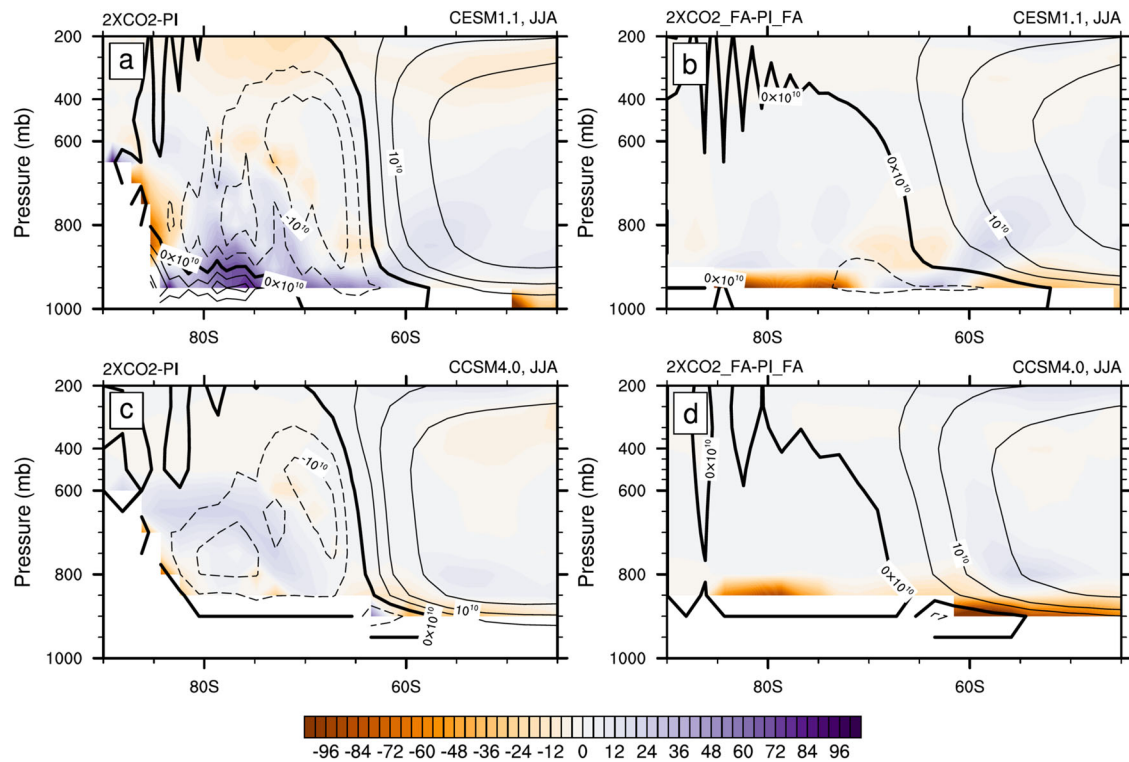


**Fig. 7 Mass overturning streamfunction and temperature advection change with CO<sub>2</sub>-doubling.** Mean meridional mass overturning streamfunction (contours; in kg per sec) and change in temperature advection with CO<sub>2</sub>-doubling (colors; in Km s<sup>-1</sup>) in the **a, b** CESM1.1 and **c, d** CCSM4.0 when **a, c** Antarctic orography is at its present-day height, 2 × CO<sub>2</sub> minus PI, and when **b, d** Antarctic orography is flattened to 10% of its present-day height, 2 × CO<sub>2</sub>\_FA minus PI\_FA. The mass overturning streamfunction is shown for the corresponding pre-industrial experiment (PI or PI\_FA).

with realistic models have convincingly shown that ozone depletion (which increases the amount of shortwave radiation reaching the surface) has in fact contributed to warmer SSTs and decreased sea ice extent<sup>44–49</sup>.

Other studies have highlighted the existence of a negative greenhouse effect over the Antarctic continent: the instantaneous outgoing longwave radiation at the top-of-atmosphere increases, rather than decreases, with higher levels of atmospheric CO<sub>2</sub><sup>50–52</sup>. That negative greenhouse effect, which only occurs in some months of the year, owes its existence to the tropospheric temperature inversion over the extremely cold Antarctic surface, and is enhanced by the relative absence of tropospheric water vapor in that region<sup>53</sup>. While that negative greenhouse effect has indeed been observed from satellites (as documented by<sup>53</sup>), it dissipates rapidly following abrupt CO<sub>2</sub>-quadrupling in fully coupled GCMs due to fast stratospheric adjustments<sup>54</sup>, and does not result in a cooling of the Antarctic surface. Furthermore, Flanner et al.<sup>55</sup> show that the net surface longwave radiative impact of greenhouse gases will always tend to heat the surface at high latitudes because of the local temperature inversion, regardless of whether the greenhouse effect is positive or negative at the top-of-atmosphere. In the present study, we do find that the net (downward) surface longwave flux with CO<sub>2</sub>-doubling is greater when Antarctic orography is flattened. However, we are leery to attribute the surface-amplified warming with flat orography to this factor: analysis of surface radiative kernels indicates that anomalies in the downward longwave flux at the surface primarily arise as a consequence of surface temperature anomalies, rather being the cause of those anomalies<sup>56</sup>. A thorough assessment of instantaneous radiative forcing, and of the accompanying rapid adjustments, is outside the scope of the present study, as we are here interested in the Antarctic surface climate response to CO<sub>2</sub>-doubling at quasi-equilibrium,

not in the details of the radiative forcing and adjustment immediately following the doubling of CO<sub>2</sub>.

We conclude by acknowledging some important caveats on the results presented here. First, we have only used two models in our study, and a more extensive model intercomparison may identify additional mechanisms that contribute to a reduction of Antarctic continental warming under CO<sub>2</sub>-forcing. Furthermore, we reiterate that although models generally agree on the local dynamic atmospheric impacts of Antarctic orography flattening, there is little intermodel agreement regarding the remote impacts of Antarctic orography flattening. For example, some GCMs simulate a global mean cooling when Antarctic orography is flattened<sup>22</sup>, while other GCMs simulate a global mean warming<sup>57</sup>, suggesting a large intermodel spread in the global radiative forcing that accompanies Antarctic orography changes. We expect that major difference across models in the global radiative forcing associated with flattening of Antarctic orography may also result in differences in the global CO<sub>2</sub>-doubling response when Antarctic orography is flattened, as we have noted above. Despite these caveats, we believe that the mechanisms we proposed in this study are likely to be robust, in that they depend on changes in local atmospheric dynamics circa the Antarctic continent, which are known to be consistent across a range of models.

## METHODS

### GCM experiments

We utilize two state-of-the-art, fully-coupled GCMs: the Community Climate System Model, version 4.0 (CCSM4.0; see ref. <sup>58</sup>), and the Community Earth System Model, version 1.1 (CESM1.1; see ref. <sup>59</sup>). The primary difference between the two GCMs is in the atmosphere model component: CCSM4.0 utilizes version 4 of the Community Atmosphere Model (CAM4<sup>60</sup>) at 2° spatial resolution, while CESM1.1 utilizes version 5

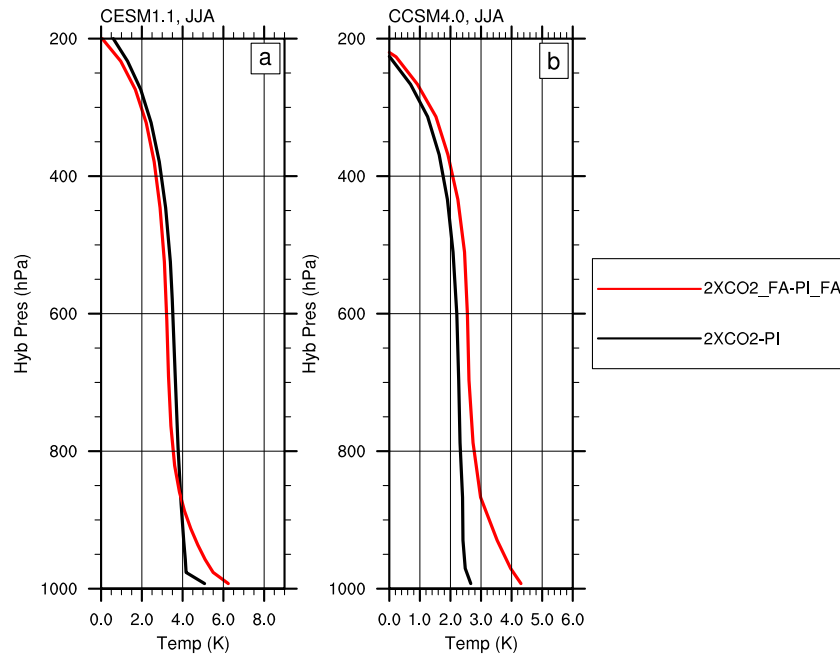


**Fig. 8 Atmospheric temperature change with CO<sub>2</sub>-doubling.** Change in the vertical profile of warming over the Antarctic continent in the **a** CESM1.1 and **b** CCSM4.0 when Antarctic orography is at its present-day elevation (solid black lines) and when Antarctic orography is flattened to 10% of its present-day elevation (dashed red lines). The vertical coordinate is a hybrid-sigma coordinate, used for ease of comparison between the present-day and flattened orography experiments.

**Table 1.** Eight GCM runs utilized in this study.

| Model   | Experiment   | Antarctic Orography | Atm CO <sub>2</sub> (ppm) | Component Set & Configuration        |
|---------|--|---------------------|---------------------------|--------------------------------------|
| CCSM4.0 | Control (PI)   | Present-day         | 284                       | b40.1850.track1.2 deg <sup>58</sup>  |
|         | CO <sub>2</sub> -doubling (2 × CO <sub>2</sub> )                     | Present-day         | 568                       |                                      |
|         | Flat Antarctic (PI_FA)   | 10% of Present-day  | 284                       |                                      |
|         | Flat Antarctic + CO <sub>2</sub> -doubling (2 × CO <sub>2</sub> _FA) | 10% of Present-day  | 568                       |                                      |
| CESM1.1 | Control (PI)   | Present-day         | 284                       | b.e11.B1850C5CN.f09g16 <sup>67</sup> |
|         | CO <sub>2</sub> -doubling (2 × CO <sub>2</sub> )                     | Present-day         | 568                       |                                      |
|         | Flat Antarctic (PI_FA)   | 10% of Present-day  | 284                       |                                      |
|         | Flat Antarctic + CO <sub>2</sub> -doubling (2 × CO <sub>2</sub> _FA) | 10% of Present-day  | 568                       |                                      |

(CAM5<sup>61</sup>) at 1° spatial resolution. CAM4 and CAM5 implement different atmospheric cloud, convection, boundary layer (including gravity wave drag), and precipitation parameterizations; as a result, the mean state climate and climate sensitivity of these two models differ significantly<sup>62</sup>.

Other than the atmosphere model, all other components are nearly identical between CCSM4.0 and CESM1.1. Both models utilize the fully dynamic CICE4 sea ice component<sup>63</sup> and the POP2 ocean component<sup>64</sup> with an isopycnal mixing parameterization to capture transport from sub-grid scale eddies<sup>65</sup>. Both ocean and sea ice are run on the same (nominally) 1° spatial resolution grid with the North Pole singularity centered over Greenland. Also, the land component for both CCSM4.0 and CESM1.1 is the CLM4<sup>66</sup>, which is run at the same resolution as the respective atmosphere model (i.e., 2° for CCSM4.0 and 1° for CESM1.1).

For both models, we perform a set of four runs: (1) a pre-industrial control experiment with present-day Antarctic orography (PI); (2) a pre-industrial control experiment with flattened Antarctic orography (PI\_FA); (3) a CO<sub>2</sub>-doubling experiment with present-day Antarctic orography (2 × CO<sub>2</sub>); and (4) a CO<sub>2</sub>-doubling experiment with flattened Antarctic orography (2 × CO<sub>2</sub>\_FA). For both models, the pre-industrial control experiment with present-day Antarctic orography (PI) was obtained from a millennium-length, publicly available, equilibrated run (see Table 1, Component Set and Configuration). Each of the other experiments were branched from this equilibrated pre-industrial control run, and integrated for a total of 230 model years with the modifications noted: CO<sub>2</sub>-doubling

(atmospheric CO<sub>2</sub> concentrations abruptly doubled from 284 to 568 ppm at the beginning of the experiment), Antarctic orography flattening (reduction of Antarctic orography to 10% of its present-day elevation at the beginning of the experiment), or both CO<sub>2</sub>-doubling and orography flattening. The details of each experiment are shown in Table 1.

Annual and seasonal climatologies are calculated using the final 30 years of each experiment. The net top-of-atmosphere anomalies for all experiments are given in Supplementary Table 1. For each model, the CO<sub>2</sub>-forced response is computed as the difference between the 2 × CO<sub>2</sub> and PI runs, either with present-day Antarctic orography (i.e., 2 × CO<sub>2</sub> minus PI) or with flattened Antarctic orography (i.e., 2 × CO<sub>2</sub>\_FA minus PI\_FA); the former shows the climate response to CO<sub>2</sub>-doubling when Antarctic orography is at its present-day elevation, and the latter shows the climate response to CO<sub>2</sub>-doubling with flattened Antarctic orography.

#### DATA AVAILABILITY

Global climate model data generated for this study are available at <https://doi.org/10.5281/zenodo.3998429>.

Received: 16 December 2019; Accepted: 10 September 2020;  
Published online: 08 October 2020

## REFERENCES

1. Rietbroek, R., Brunnabend, S.-E., Kusche, J., Schröter, J. & Dahle, C. Revisiting the contemporary sea-level budget on global and regional scales. *Proc. Natl Acad. Sci. USA* **113**, 1504–1509 (2016).
2. Atkinson, A., Siegel, V., Pakhomov, E. & Rothery, P. Long-term decline in krill stock and increase in salps within the Southern Ocean. *Nature* **432**, 100–103 (2004).
3. McGraw, M. & Barnes, E. Seasonal sensitivity of the eddy-driven jet to tropospheric heating in an idealized AGCM. *J. Clim.* **29**, 5223–5240 (2016).
4. Chiang, J. C. & Bitz, C. M. Influence of high latitude ice cover on the marine intertropical convergence zone. *Clim. Dyn.* **25**, 477–496 (2005).
5. Comiso, J. C. & Hall, D. K. Climate trends in the arctic as observed from space. *Wiley Interdiscip. Rev. Clim. Chang.* **5**, 389–409 (2014).
6. Screen, J. & Simmonds, I. The central role of diminishing sea ice in recent Arctic temperature amplification. *Nature* **464**, 1334–1337 (2010).
7. Screen, J. & Simmonds, I. Increasing fall–winter energy loss from the Arctic Ocean and its role in Arctic temperature amplification. *Geophys. Res. Lett.* **37**, L16707 (2010).
8. Hwang, Y.-T., Frierson, D. & Kay, J. Coupling between Arctic feedbacks and changes in poleward energy transport. *Geophys. Res. Lett.* **38**, L17704 (2011).
9. Graversen, R. G., Langen, P. L. & Mauritsen, T. Polar amplification in CCSM4: contributions from the lapse rate and surface albedo feedbacks. *J. Clim.* **27**, 4433–4450 (2014).
10. Pithan, F. & Mauritsen, T. Arctic amplification dominated by temperature feedbacks in contemporary climate models. *Nat. Geosci.* **7**, 181 (2014).
11. Vose, R. S. et al. NOAA's merged land–ocean surface temperature analysis. *Bull. Am. Meteorol. Soc.* **93**, 1677–1685 (2012).
12. Parkinson, C. & Cavalieri, D. Antarctic sea ice variability and trends, 1979–2010. *Cryosphere* **6**, 871–880 (2012).
13. Smith, K. L. & Polvani, L. M. Spatial patterns of recent Antarctic surface temperature trends and the importance of natural variability: lessons from multiple reconstructions and the CMIP5 models. *Clim. Dyn.* **48**, 2653–2670 (2017).
14. Mechoso, C. Topographic influences on the general circulation of the Southern Hemisphere: a numerical experiment. *Mon. Weather. Rev.* **109**, 2131–2139 (1981).
15. Parish, T. On the role of Antarctic katabatic winds in forcing large-scale tropospheric motions. *J. Atmos. Sci.* **49**, 1374–1385 (1991).
16. Egger, J. Topographic wave modification and the angular momentum balance of the Antarctic troposphere. *J. Atmos. Sci.* **49**, 327–334 (1992).
17. Parish, T., Bromwich, D. & Tzeng, R.-Y. On the role of the Antarctic continent in forcing large-scale circulations in the high southern latitudes. *J. Atmos. Sci.* **51**, 3566–3579 (1994).
18. Egger, J. Antarctic slope winds and the polar stratospheric vortex. *J. Atmos. Terr. Phys.* **56**, 1067–1072 (1994).
19. Ogura, T. & Abe-Ouchi, A. Influence of the Antarctic ice sheet on southern high latitude climate during the Cenozoic: albedo vs topography effect. *Geophys. Res. Lett.* **28**, 587–590 (2001).
20. Mechoso, C. The atmospheric circulation around Antarctica: linear stability and finite amplitude interactions with migrating cyclones. *J. Atmos. Sci.* **37**, 2209–2233 (1980).
21. Walsh, K., Simmonds, I. & Collier, M. Sigma-coordinate calculation of topographically forced baroclinicity around Antarctica. *Dyn. Atmos. Ocean.* **33**, 1–29 (2000).
22. Singh, H., Bitz, C. & Frierson, D. The global climate response to lowering surface orography of Antarctica and the importance of atmosphere–ocean coupling. *J. Clim.* **29**, 4137–4153 (2016).
23. Salzmann, M. The polar amplification asymmetry: role of Antarctic surface height. *Earth Syst. Dyn.* **8**, 323–336 (2017).
24. Hwang, Y.-T. & Frierson, D. Increasing atmospheric poleward energy transport with global warming. *Geophys. Res. Lett.* **37**, L24807 (2010).
25. Held, I. & Soden, B. Robust responses of the hydrological cycle to global warming. *J. Clim.* **19**, 5686–5699 (2006).
26. Pauluis, O., Czaja, A. & Korty, R. The global atmospheric circulation on moist isentropes. *Science* **321**, 1075–1078 (2008).
27. Pauluis, O., Czaja, A. & Korty, R. The global atmospheric circulation in moist isentropic coordinates. *J. Clim.* **23**, 3077–3093 (2010).
28. Bailey, A., Singh, H. K. & Nusbaumer, J. Evaluating a moist isentropic framework for poleward moisture transport: implications for water isotopes over Antarctica. *Geophys. Res. Lett.* **46**, 7819–7827 (2019).
29. Deser, C., Tomas, R., Alexander, M. & Lawrence, D. The seasonal atmospheric response to projected Arctic sea ice loss in the late twenty-first century. *J. Clim.* **23**, 333–351 (2010).
30. Manabe, S. & Wetherald, R. The effects of doubling the CO<sub>2</sub> concentration on the climate of a general circulation model. *J. Atmos. Sci.* **32**, 3–15 (1975).
31. Soden, B., Held, I., Colman, R., Shell, K. & Kiehl, J. Quantifying climate feedbacks using radiative kernels. *J. Clim.* **21**, 3504–3520 (2008).
32. Shell, K., Kiehl, J. & Shields, C. Radiative kernel technique to calculate climate feedbacks in NCAR's Community Atmospheric Model. *J. Clim.* **21**, 2269–2283 (2008).
33. Bintanja, R., Graverson, R. & Hazeleger, W. Arctic winter warming amplified by the thermal inversion and consequent low infrared cooling to space. *Nat. Geosci.* **4**, 758–760 (2011).
34. Feldl, N., Anderson, B. T. & Bordoni, S. Atmospheric eddies mediate lapse rate feedback and Arctic amplification. *J. Clim.* **30**, 9213–9224 (2017).
35. Holland, M. & Bitz, C. Polar amplification of climate change in coupled models. *Clim. Dyn.* **21**, 221–232 (2003).
36. Singh, H., Rasch, P. & Rose, B. Increased ocean heat convergence into the high latitudes with CO<sub>2</sub> doubling enhances polar-amplified warming. *Geophys. Res. Lett.* **44**, 10583–10591 (2017).
37. Armour, K., Marshall, J., Scott, J., Donohoe, A. & Newsom, E. Southern Ocean warming delayed by circumpolar upwelling and equatorward transport. *Nat. Geosci.* **9**, 549–554 (2016).
38. Stocker, T. et al. Technical Summary, Climate Change 2013: The Physical Science Basis. Contribution of Working Group I to the Fifth Assessment Report of the Intergovernmental Panel on Climate Change, Book Section TS, 33–115 (Cambridge University Press, Cambridge, United Kingdom and New York, NY, USA, 2013).
39. Noone, D. & Simmonds, I. Annular variations in moisture transport mechanisms and the abundance of  $\delta$  18o in Antarctic snow. *J. Geophys. Res. Atmos.* **107**, ACL–3 (2002).
40. Noone, D. The influence of midlatitude and tropical overturning circulation on the isotopic composition of atmospheric water vapor and Antarctic precipitation. *J. Geophys. Res. Atmos.* **113**, D04102 (2008).
41. Ferreira, D., Marshall, J., Bitz, C. M., Solomon, S. & Plumb, A. Antarctic ocean and sea ice response to ozone depletion: a two-time-scale problem. *J. Clim.* **28**, 1206–1226 (2015).
42. Polvani, L. M., Waugh, D. W., Correa, G. J. & Son, S.-W. Stratospheric ozone depletion: the main driver of twentieth-century atmospheric circulation changes in the southern hemisphere. *J. Clim.* **24**, 795–812 (2011).
43. Marshall, J. et al. The ocean's role in polar climate change: asymmetric Arctic and Antarctic responses to greenhouse gas and ozone forcing. *Philos. Trans. R. Soc. A* **372**, 20130040 (2014).
44. Sigmond, M. & Fyfe, J. Has the ozone hole contributed to increased Antarctic sea ice extent? *Geophys. Res. Lett.* **37**, L18502 (2010).
45. Bitz, C. & Polvani, L. M. Antarctic climate response to stratospheric ozone depletion in a fine resolution ocean climate model. *Geophys. Res. Lett.* **39**, L20705 (2012).
46. Sigmond, M. & Fyfe, J. C. The Antarctic sea ice response to the ozone hole in climate models. *J. Clim.* **27**, 1336–1342 (2014).
47. Solomon, A., Polvani, L. M., Smith, K. & Abernathy, R. The impact of ozone depleting substances on the circulation, temperature, and salinity of the southern ocean: an attribution study with cesm1 (waccm). *Geophys. Res. Lett.* **42**, 5547–5555 (2015).
48. Landrum, L. L., Holland, M. M., Raphael, M. N. & Polvani, L. M. Stratospheric ozone depletion: an unlikely driver of the regional trends in Antarctic sea ice in Austral fall in the late twentieth century. *Geophys. Res. Lett.* **44**, 11–062 (2017).
49. Seviour, W. et al. The Southern Ocean sea surface temperature response to ozone depletion: a multimodel comparison. *J. Clim.* **32**, 5107–5121 (2019).
50. Huang, Y., Tan, X. & Xia, Y. Inhomogeneous radiative forcing of homogeneous greenhouse gases. *J. Geophys. Res. Atmos.* **121**, 2780–2789 (2016).
51. Schmithüsen, H., Notholt, J., König-Langlo, G., Lemke, P. & Jung, T. How increasing CO<sub>2</sub> leads to an increased negative greenhouse effect in Antarctica. *Geophys. Res. Lett.* **42**, 10–422 (2015).
52. Sejas, S. A., Cai, M., Liu, G., Taylor, P. C. & Tung, K.-K. A Lagrangian view of longwave radiative fluxes for understanding the direct heating response to a CO<sub>2</sub> increase. *J. Geophys. Res. Atmos.* **121**, 6191–6214 (2016).
53. Sejas, S. A., Taylor, P. C. & Cai, M. Unmasking the negative greenhouse effect over the Antarctic Plateau. *npj Clim. Atmos. Sci.* **1**, 1–9 (2018).
54. Smith, K. L., Chiodo, G., Previdi, M. & Polvani, L. M. No surface cooling over Antarctica from the negative greenhouse effect associated with instantaneous quadrupling of CO<sub>2</sub> concentrations. *J. Clim.* **31**, 317–323 (2018).
55. Flanner, M., Huang, X., Chen, X. & Krinner, G. Climate response to negative greenhouse gas radiative forcing in polar winter. *Geophys. Res. Lett.* **45**, 1997–2004 (2018).
56. Vargas Zeppetello, L., Donohoe, A. & Battisti, D. Does surface temperature respond to or determine downwelling longwave radiation? *Geophys. Res. Lett.* **46**, 2781–2789 (2019).
57. Justino, F. et al. Influence of Antarctic ice sheet lowering on the Southern Hemisphere climate: modeling experiments mimicking the mid-Miocene. *Clim. Dyn.* **42**, 843–858 (2014).
58. Gent, P. R. et al. The Community Climate System Model version 4. *J. Clim.* **24**, 4973–4991 (2011).
59. Hurrell, J. et al. The Community Earth System Model: a framework for collaborative research. *Bull. Am. Meteorol. Soc.* **94**, 1339–1360 (2013).

60. Neale, R. B. et al. The mean climate of the Community Atmosphere Model (CAM4) in forced SST and fully coupled experiments. *J. Clim.* **26**, 5150–5168 (2013).
61. Neale, R. et al. Description of NCAR Community Atmosphere Model (CAM 5.0). NCAR Technical Note TN-486 + STR, NCAR (2012).
62. Meehl, G. A. et al. Climate change projections in CESM1 (CAM5) compared to CCSM4. *J. Clim.* **26**, 6287–6308 (2013).
63. Hunke, E. & Lipscomb, W. CICE: the Los Alamos sea ice model, documentation and software, version 4.0. Technical Report LA-CC-06-012. (Los Alamos National Laboratory, 2008).
64. Danabasoglu, G. et al. The CCSM4 ocean component. *J. Clim.* **25**, 1361–1389 (2012).
65. Gent, P. & McWilliams, J. Isopycnal mixing in ocean circulation models. *J. Phys. Oceanogr.* **20**, 150–155 (1992).
66. Oleson, K. et al. Technical description of version 4.0 of the Community Land Model (CLM). Technical Report TN-478 + STR. (National Center for Atmospheric Research, 2010).
67. Kay, J. et al. The Community Earth System Model (CESM) Large Ensemble project: a community resource for studying climate change in the presence of internal climate variability. *Bull. Am. Meteorol. Soc.* **96**, 1333–1349 (2015).

## ACKNOWLEDGEMENTS

H.A.S. acknowledges funding and computing support from the Linus Pauling Distinguished Postdoctoral Fellowship at the Pacific Northwest National Laboratory, sponsored by the US Department of Energy Office of Science. L.M.P. is funded, in part, by a grant from the US National Science Foundation (OPP-1745029) to Columbia University.

## AUTHOR CONTRIBUTIONS

H.A.S. and L.M.P. conceived and planned the project. H.A.S. carried out the numerical experiments and analyzed the model output. H.A.S. wrote the first draft, and both authors contributed to the final version of the paper.

## COMPETING INTERESTS

The authors declare no competing interests.

## ADDITIONAL INFORMATION

**Supplementary information** is available for this paper at <https://doi.org/10.1038/s41612-020-00143-w>.

**Correspondence** and requests for materials should be addressed to H.A.S.

**Reprints and permission information** is available at <http://www.nature.com/reprints>

**Publisher's note** Springer Nature remains neutral with regard to jurisdictional claims in published maps and institutional affiliations.



**Open Access** This article is licensed under a Creative Commons Attribution 4.0 International License, which permits use, sharing, adaptation, distribution and reproduction in any medium or format, as long as you give appropriate credit to the original author(s) and the source, provide a link to the Creative Commons license, and indicate if changes were made. The images or other third party material in this article are included in the article's Creative Commons license, unless indicated otherwise in a credit line to the material. If material is not included in the article's Creative Commons license and your intended use is not permitted by statutory regulation or exceeds the permitted use, you will need to obtain permission directly from the copyright holder. To view a copy of this license, visit <http://creativecommons.org/licenses/by/4.0/>.

© The Author(s) 2020, corrected publication 2021